JOURNAL OF BACTERIOLOGY, Sept. 1998, p. 4903–4911 Vol. 180, No. 18
0021-9193/98/$04.00+0


# Two Functionally Distinct Regions Upstream of the $cbb_I$ Operon of *Rhodobacter sphaeroides* Regulate Gene Expression

JAMES M. DUBBS AND F. ROBERT TABITA*

*Department of Microbiology and the Plant Molecular Biology/Biotechnology Program, The Ohio State University, Columbus, Ohio 43210-1292*

Received 30 December 1997/Accepted 21 July 1998

**A number of $cbbF_I$::*lacZ* translational fusion plasmids containing various lengths of sequence 5′ to the form I ($cbb_I$) Calvin-Benson-Bassham cycle operon ($cbbF_IcbbP_IcbbA_IcbbL_IcbbS_I$) of *Rhodobacter sphaeroides* were constructed. Expression of β-galactosidase was monitored under a variety of growth conditions. It was found that 103 bp of sequence upstream of the $cbbF_I$ transcription start was sufficient to confer low levels of regulated $cbb_I$ promoter expression; this activity was dependent on the presence of an intact *cbbR* gene. Additionally, *R. sphaeroides* CbbR was shown to bind to the region between 9 and 100 bp 5′ to the $cbbF_I$ transcription start. Inclusion of an additional upstream sequence, from 280 to 636 bp 5′ to $cbbF_I$, resulted in a significant increase in regulated $cbb_I$ promoter expression under all growth conditions tested. A 50-bp region responsible for the majority of this increase occurs between 280 and 330 bp 5′ to $cbbF_I$. The additional 306 bp of upstream sequence from 330 to 636 bp also appears to play a positive regulatory role. A 4-bp deletion 281 to 284 bp 5′ to $cbbF_I$ significantly reduced $cbb_I$ expression while the proper regulatory pattern was retained. These studies provide evidence for the presence of two functionally distinct regions of the $cbb_I$ promoter, with the distal domain providing significant regulated promoter activity that adheres to the normal pattern of expression.**

Nonsulfur purple bacteria are capable of growth under a variety of physiological conditions (26). Under growth conditions where $CO_2$ functions as the sole carbon source (i.e., chemo- and photoautotrophic conditions), the Calvin-Benson-Bassham (CBB) cycle is essential for providing virtually all cellular carbon (39). When fixed carbon sources are available, the CBB cycle functions as a minor carbon assimilatory pathway, with $CO_2$ used primarily as a terminal electron acceptor (43). *Rhodobacter sphaeroides* is an excellent model system to study the control of CBB cycle (*cbb*) gene expression due to the fact that this organism reversibly regulates the expression of two major *cbb* operons. The form I ($cbb_I$) and form II ($cbb_{II}$) operons (12, 17) are located on two separate genetic elements (chromosome I and chromosome II, respectively) of this organism (36, 37). The $cbb_I$ operon is comprised of the *cbbFPALS* structural genes that encode, respectively, the CBB cycle enzymes fructose 1,6-sedoheptulose 1,7-bisphosphatase ($cbbF_I$), phosphoribulokinase ($cbbP_I$), and fructose 1,6-sedoheptulose 1,7-bisphosphate aldolase ($cbbA_I$), as well as the large- and small-subunit genes of form I ($L_8S_8$) ribulose-1,5-bisphosphate carboxylase oxygenase (RubisCO) ($cbbL_IcbbS_I$) (15). The $cbb_{II}$ operon is similar to the $cbb_I$ operon, but in addition to similar, but not identical, copies of the F, P, and A genes, this cluster contains genes encoding transketolase ($cbbT_{II}$) and glyceraldehyde-3-phosphate dehydrogenase ($cbbG_{II}$) and the gene encoding the single large-type subunit of the distinct form II-type RubisCO ($cbbM_{II}$) (4). Mutagenesis studies indicate that the genes of the $cbb_I$ and $cbb_{II}$ clusters are each controlled by single promoters 5′ to the first gene of the respective operon (4, 14, 15). Studies at the protein level have shown that regulation of expression of these structural genes is complex in *R. sphaeroides*. During aerobic chemoheterotrophic growth, the expression of both *cbb* operons is repressed. Under photosynthetic growth conditions, expression of both the $cbb_I$ and $cbb_{II}$ operons is derepressed, with each operon independently responding to a number of environmental signals such as the $CO_2$ concentration and the redox state of the fixed carbon compounds supplied for growth (8, 13, 19, 20, 22). Photoheterotrophic growth results in expression of both operons with the $cbb_{II}$ gene products generally predominating, resulting in a form I-to-form II RubisCO ratio of approximately 1:2 (22). The overall level of gene expression during photoheterotrophic growth is affected by the redox state of the carbon source supplied for growth, with more-reduced carbon sources resulting in higher levels of *cbb* gene expression (38). Maximal expression from both operons occurs under photoautotrophic conditions (in a 1.5% $CO_2$–98.5% $H_2$ atmosphere); however, under these conditions expression of the $cbb_I$ operon predominates over that of the $cbb_{II}$ operon. This differential expression of the two operons led to the proposal that form II RubisCO functions primarily as a terminal electron acceptor, maintaining the redox balance of the cell, while the function of the form I enzyme is to provide the cell with fixed carbon (17, 19, 43). While both the *cbb* operons display independent regulation, results of mutagenesis studies indicate that there is communication between the two operons. Insertional mutagenesis of genes in either operon gives rise to a compensatory increase in the expression of the unaffected operon, resulting in enzyme levels that are equal to or higher than those of wild-type cells (8, 15, 19, 20). This compensatory effect is mediated by the *cbbR* gene, which is divergently transcribed from $cbbF_I$ (16). CbbR was thus found to be a positive regulator of both operons. *cbb* gene expression in a number of other aerobic and anaerobic autotrophic bacteria has also been shown to be influenced by the product of the *cbbR* gene (10, 24, 28, 40, 42, 46), and CbbR was found to bind specifically to AT-rich sites within the *cbbR-cbbL* intergenic regions of *Ralstonia eutropha* (*Alcaligenes eutrophus*) (25) and *Xanthobacter flavus* (41) as well as *Chromatium vinosum* (42) and *Thiobacillus ferrooxidans* (24).

As a first step in the identification of DNA sequences in-

* Corresponding author. Mailing address: Department of Microbiology, The Ohio State University, 484 West 12th Ave., Columbus, OH 43210-1292. Phone: (614) 292-4297. Fax: (614) 292-6337. E-mail: Tabita.1@osu.edu.

TABLE 1. Strains and plasmids

| Plasmid or strain | Relevant characteristics | Reference or source |
|---|---|---|
| pK18 | $Km^r$; derivative of pUC18 | 32 |
| pKC1-5 | $Km^r$; pK18 containing the 719-bp *Eco*RI-*Ava*II fragment of pUC12EH | This study |
| pKC1ΔXho | $Km^r$; pKC1-5 containing a 4-bp deletion at the *Xho*I site within the insert | This study |
| p12EH | $Ap^r$; pUC9 carrying a 1.8-kbp *Eco*RI-*Hin*dIII fragment containing *cbbR* | 16 |
| pMC1403 | $Ap^r$; LacZ translational fusion vector | 34 |
| pMC1H1 | $Ap^r$; pMC1403 carrying the 187-bp *Bss*HII-*Bam*HI fragment of pKC1-5 | This study |
| pMCB1 | $Ap^r$; pMC1403 carrying the 363-bp *Xho*I-*Bam*HI fragment of pKC1-5 | This study |
| pMCG1 | $Ap^r$; pMC1403 carrying the 413-bp *Pfl*MI-*Bam*HI fragment of pKC1-5 | This study |
| pMCG1ΔXho | $Ap^r$; pMCG1 carrying a 4-bp deletion at the *Xho*I site | This study |
| pMCF1 | $Ap^r$; pMC1403 carrying the 584-bp *Dra*III-*Bam*HI fragment of pKC1-5 | This study |
| pMCE1 | $Ap^r$; pMC1403 carrying the 674-bp *Nar*I-*Bam*HI fragment of pKC1-5 | This study |
| pMCC1 | $Ap^r$; pMC1403 carrying the 719-bp *Eco*RI-*Bam*HI fragment of pKC1-5 | This study |
| pMCC1ΔXho | $Ap^r$; pMCC1 carrying a 4-bp deletion at the *Xho*I site | This study |
| pMCD1 | $Ap^r$; pMC1403 carrying the 1,323-bp *Hin*dIII-*Ava*II fragment of p12EH | This study |
| pVK101 | $Km^r$ $Tc^r$; broad-host-range vector | 23 |
| pVK1403 | $Ap^r$; pVK101 containing pMC1403 inserted in the *Eco*RI site | This study |
| pVKH1 | $Km^r$ $Tc^r$ $Ap^r$; pVK101 carrying pMCH1 inserted in the *Eco*RI site | This study |
| pVKB1 | $Km^r$ $Tc^r$ $Ap^r$; pVK101 carrying pMCB1 inserted in the *Eco*RI site | This study |
| pVKG1 | $Km^r$ $Tc^r$ $Ap^r$; pVK101 carrying pMCG1 inserted in the *Eco*RI site | This study |
| pVKG1ΔXho | $Km^r$ $Tc^r$ $Ap^r$; pVK101 carrying pMCG1ΔXho inserted in the *Eco*RI site | This study |
| pVKF1 | $Km^r$ $Tc^r$ $Ap^r$; pVK101 carrying pMCF1 inserted in the *Eco*RI site | This study |
| pVKE1 | $Km^r$ $Tc^r$ $Ap^r$; pVK101 carrying pMCE1 inserted in the *Eco*RI site | This study |
| pVKC1 | $Km^r$ $Tc^r$ $Ap^r$; pVK101 carrying pMCC1 inserted in the *Eco*RI site | This study |
| pVKC1ΔXho | $Km^r$ $Tc^r$ $Ap^r$; pVK101 carrying pMCC1ΔXho inserted in the *Eco*RI site | This study |
| pVKD1 | $Km^r$ $Tc^r$ $Ap^r$; pVK101 carrying pMCD1 inserted in the *Eco*RI site | This study |
| pRK2013 | $Km^r$; conjugative helper plasmid | 11 |
| pET11a | $Ap^r$; *E. coli* expression vector | 7 |
| pET11R-11 | $Ap^r$; pET11a carrying a 1,045-bp *Nde*I-*Bam*HI fragment spanning *cbbR* | This study |
| *R. sphaeroides* strains | | |
| HR | Wild type; $Sm^r$ | 44 |
| 1312 | *cbbR*::$Tp^r$ | 16 |
| CAC | Chemoautotrophic-competent variant of *R. sphaeroides* HR | 31 |
| *E. coli* strains | | |
| JM109 | | 47 |
| MM294 | | 11 |
| BL21(DE3) | Expression strain carrying an IPTG-inducible T7 RNA polymerase gene | 35 |

volved in the regulation of $cbb_I$ operon expression, we have constructed $cbb_I$::*lacZ* translational fusions and monitored their expression under a variety of growth conditions. In this communication, we identified a region of sequence 5′ to $cbbF_I$ involved in *cbbR*-dependent regulation of the $cbb_I$ operon. We show that CbbR binds to this region in vitro. We also demonstrate that an additional upstream region is necessary for high levels of $cbb_I$ expression.

## MATERIALS AND METHODS

**Bacterial strains, plasmids, and culture conditions.** All bacterial strains and plasmids used in this study are described in Table 1. *Escherichia coli* JM109 was used to maintain all plasmids, with the exception of pRK2013, which was maintained in *E. coli* MM294. *E. coli* BL21(DE3) (35) was used as the host for expression of *R. sphaeroides* CbbR from the plasmid pET11R-11. Anaerobic growth of *E. coli* was achieved under an atmosphere of 100% argon. *R. sphaeroides* strains were grown photoheterotrophically and photoautotrophically under a 1.5% $CO_2$–98.5% $H_2$ atmosphere as previously described (22). Aerobic chemoheterotrophic growth was performed with Omerod's medium (29) supplemented with 0.4% malate while the culture was shaken vigorously in the dark at 30°C. Chemoautotrophic cultures received a gas atmosphere of 5% $CO_2$–45% $H_2$–50% air. Antibiotics were added to the medium, as required, at the indicated concentrations (micrograms per milliliter): for *E. coli*, ampicillin (100), tetracycline (12.5), and kanamycin (50); for *R. sphaeroides*, tetracycline (12.5), kanamycin (50), and trimethoprim (200).

**DNA manipulations and sequencing.** Plasmid isolations and transformations were performed by standard procedures. DNA sequencing of plasmid subclones was performed by the dideoxy chain termination method on base denatured plasmid templates as described elsewhere (3). Plasmid templates were purified by CsCl-ethidium bromide centrifugation (27).

**Construction of $cbbF_I$::*lacZ* fusion plasmids.** All fusion plasmid constructions made use of the *Ava*II site located at a position 56 bp within $cbbF_I$ in plasmid p12EH, as well as a number of upstream sites (see Fig. 2). Each fragment was isolated, and either it was digested with mung bean nuclease (BRL, Gaithersburg, Md.) to remove overhanging ends or the ends were filled in with Klenow polymerase and deoxynucleoside triphosphates. The fragment was then ligated into the translational fusion vector pMC1403 (34) to generate an in-frame fusion of $cbbF_I$ with *lacZ*. The pMC1403-$cbbF_I$ fusion was then linearized by digestion with *Eco*RI and ligated into the *Eco*RI site of the conjugative plasmid pVK101 (23). This final construct could then be mated into *R. sphaeroides*. The 4-bp deletion of plasmid pVKC1ΔXho was constructed by digestion of plasmid pKC1-5 with *Xho*I followed by digestion with mung bean nuclease and religation to create plasmid pKC1ΔXho. The *Eco*RI/*Bam*HI insert of pKC1ΔXho was then cloned into pMC1403, followed by ligation into the *Eco*RI site of pVK101. The copy number of pVK101 in *R. sphaeroides* is not known; however, the copy number of the related RK2 derivative pRK404 has been reported as four to six copies per chromosome, under phototrophic growth conditions (5).

**Immunological techniques and RubisCO assays.** Cell extracts were prepared as previously described (9), and RubisCO activity was determined by a radiometric method (45). Rocket immunoelectrophoresis was performed as previously described (22) with antibodies directed against form I and form II RubisCO. Total protein was determined with the Bio-Rad protein assay dye binding reagent (Bio-Rad Laboratories, Hercules, Calif.).

**β-Galactosidase assays.** Cultures of *R. sphaeroides* were grown to mid- to late exponential phase (optical density at 660 nm [$OD_{660}$] of 0.7 to 1.1). Cells were harvested and washed, and the cell pellet was then resuspended in 1 to 5 ml of cold sonication buffer (25 mM Tris-HCl [pH 7.0], 1 mM EDTA, 5 mM β-mercaptoethanol) and sonicated (four 30-s bursts) on ice. The lysate was then centrifuged for 15 min at 10,000 × *g*, the supernatant was collected, and the protein concentration was determined. β-Galactosidase assays were performed by mixing the desired volume of extract with 1 ml of Z buffer (50 mM sodium phosphate [pH 7.0], 10 mM KCl, 1 mM $MgSO_4 \cdot 7H_2O$, 50 mM β-mercaptoethanol) in a cuvette. To this cuvette, 0.2 ml of a 4-mg/ml solution of *o*-nitro-

phenyl-β-D-galactopyranoside in 0.1 M phosphate buffer (pH 7.0 to 7.5) was added. The change in absorbance over time was then monitored with a Beckman DU-70 spectrophotometer. The β-galactosidase activity (i.e., the amount of *o*-nitrophenol produced per minute per milligram of protein) was then calculated from the extinction coefficient of *o*-nitrophenol.

**RNA isolation and primer extension.** Total RNA from *R. sphaeroides* HR and *R. sphaeroides* HR::pVKC1 was isolated from 300-ml cultures grown to mid-exponential phase ($OD_{660}$ of 0.6 to 0.8) under photoautotrophic, photoheterotrophic, and chemoheterotrophic conditions, by a method previously described (6). Primer extension mapping of the 5′ endpoints of mRNA was performed by the method described by Ausubel et al. (1) and employed avian myoblastosis virus reverse transcriptase (Boehringer Mannheim Biochemicals, Indianapolis, Ind.). The aqueous hybridization option recommended for oligonucleotide primers was used. The hybridization solution contained 0.3 M NaCl, 0.5 M HEPES (pH 7.5), and 1 mM EDTA. Oligonucleotide primers with the sequences 5′-GTATGGCATCGGGGTGGGTG-3′ (cbbF1-ex), 5′-TGCGGCTCGATGCGATCACC-3′ (cbb1-10), and 5′-CCGAGACGGGCTCCTTCACG-3′ (cbb1-C) (see Fig. 1A) were used in experiments employing *R. sphaeroides* HR RNA. A *lacZ* complementary primer with the sequence 5′-CGCCAGGGTTTTCCCAG-3′ (PMC1) (see Fig. 1A) was used in experiments employing *R. sphaeroides* HR::pVKC1 RNA.

**Construction of an *R. sphaeroides cbbR* expression plasmid.** A 1,045-bp DNA fragment containing the *R. sphaeroides cbbR* was generated via PCR in which an *Nde*I site, overlapping the *cbbR* start codon, was introduced along with a *Bam*HI site 115 bp downstream of the *cbbR* translation stop. The PCR fragment was subcloned into pBS(SK−) and sequenced. The *Nde*I-*Bam*HI fragment was then ligated into *Nde*I-*Bam*HI-digested pET11a (7) to generate the plasmid pET11R-11.

**Synthesis of *R. sphaeroides* CbbR in *E. coli* and preparation of extracts.** A 300-ml culture of *E. coli* BL21(DE3) (35) carrying pET11R-11 was grown anaerobically at room temperature in Terrific broth (1.2% [wt/vol] tryptone, 2.4% [wt/vol] yeast extract in 89 mM potassium phosphate buffer [pH 7.5] supplemented with 0.4% [wt/vol] fumarate, 0.1% glycerol, and 200 μg of ampicillin per ml) to an $OD_{660}$ of 0.6. CbbR expression was induced with the addition of IPTG (isopropyl-β-D-thiogalactopyranoside) (1 mM) followed by continued incubation for 12 h. Preparation of CbbR extracts was then performed by a modification of a previously described method (2) as follows. The cells were pelleted and washed with 50 mM MOPS (morpholinepropanesulfonic acid)–KOH (pH 7.0) and frozen at −70°C. The cells were thawed and resuspended in 5 ml of buffer B (300 mM potassium glutamate, 10 mM Tris [pH 8.5], 30% glycerol, 1 mM dithiothreitol). Phenylmethylsulfonyl fluoride (1 mM) was added immediately prior to lysis via passage through a French pressure cell. Cell debris was removed via centrifugation at 12,000 × *g* for 15 min. Nucleic acids were removed from the cleared lysate through the addition of polyethyleneimine, at a ratio of 0.2 g of polyethyleneimine/g of protein, and incubation at 0°C for 10 min. The sample was centrifuged at 12,000 × *g* for 20 min, and the supernatant was subjected to ammonium sulfate precipitation at 70% saturation. The precipitated pellet was resuspended in 2 ml of buffer A (10 mM Tris-borate [pH 8.0], 10% glycerol, 1 mM dithiothreitol) containing 500 mM NaCl (A-500) and dialyzed against buffer A containing 50 mM NaCl (A-50) until a white precipitate formed. The precipitate was collected via centrifugation at 12,000 × *g* for 20 min. The pellet was resuspended in 0.5 ml of buffer A-500 and resolubilized with the addition of 2 ml of buffer A containing 1.65 M guanidine-HCl. The sample was then dialyzed exhaustively against buffer B. The sample was centrifuged at 12,000 × *g* for 10 min, and the supernatant was stored for short periods at 4°C or for longer periods at −20°C.

**Gel mobility shift assays.** Gel mobility shift assays were performed as described by Ausubel et al. (1) with the high-ionic-strength Tris-glycine gel system. CbbR-containing extract and competitor DNA were mixed in a total volume of 50 μl of buffer B and incubated for 5 min at room temperature. Radiolabeled probe DNA (~10,000 cpm) was then added, and the reaction was incubated for an additional 20 min at room temperature. Following electrophoresis, the gels were dried and the bands were visualized by a Storm 840 PhosphorImager and ImageQuant version 4.2 software (Molecular Dynamics, Inc., Sunnyvale, Calif.).

## RESULTS

**Mapping of the $cbbF_I$ mRNA start site.** Primer extension mapping experiments, with total RNA extracted from late-exponential-phase *R. sphaeroides* HR grown under photoautotrophic conditions and the oligonucleotide cbbF1-ex, indicated potential mRNA start sites at positions 27 and 19 bp upstream of the first codon of $cbbF_I$ (Fig. 1). Experiments with RNA extracted from chemoheterotrophically and photoheterotrophically grown cells yielded a start point at 19 bp 5′ to $cbbF_I$ (data not shown). No additional upstream start points that would indicate the existence of a second promoter (data not shown) could be identified with primers cbb1-10 and cbb1-C (Fig. 1A). Experiments with the *lacZ* complementary primer PMC1 (Fig. 1A) and *R. sphaeroides* HR::pVKC1 RNA detected a single mRNA start 24 bp 5′ to $cbbF_I$, indicating that transcription of the $cbb_I$::*lacZ* fusion construct initiates from approximately the same point as does that of the chromosomal $cbb_I$ operon (data not shown).

**Regulation of $cbbF_I$::*lacZ* translational fusion plasmids in *R. sphaeroides* HR.** In order to delimit the DNA sequence required for transcriptional regulation of the $cbb_I$ operon, a series of *lacZ* translational fusion plasmids containing from 103 to 1,242 bp of DNA upstream of the $cbbF_I$ transcription start were constructed (Fig. 2). These plasmids were introduced into *R. sphaeroides* HR, and the resulting strains were assayed for β-galactosidase activity under chemoheterotrophic, photoheterotrophic, and photoautotrophic growth conditions (Fig. 2A, C, and E, respectively). In all cases, there was a dramatic increase in β-galactosidase activity in cells grown under photosynthetic conditions, with $CO_2$ as the sole source of carbon (Fig. 2E), while photosynthetic growth in the presence of malate resulted in significantly lower activity (Fig. 2C). Aerobic growth in the malate medium yielded the lowest levels of *lacZ* expression with all plasmids (Fig. 2A). Close scrutiny of the results with each of the *lacZ* constructs suggested that the $cbb_I$ promoter was comprised of three domains: one within 103 bp 5′ to the $cbbF_I$ transcription start that confers the proper pattern of regulation, and a more distal region, possibly comprised of two domains, that is necessary for high levels of $cbb_I$ expression. The first putative domain is situated at or around the *Xho*I site, with the second domain being located between the *Pfl*MI and *Ava*II restriction sites.

With regard to the promoter-proximal upstream activating sequence (UAS), addition of 50 bp to plasmid pVKB1, between 280 and 330 bp upstream of the $cbbF_I$ transcription start, to create fusion plasmid pVKG1, resulted in large increases in expression under photoheterotrophic and photoautotrophic growth conditions, 9- and 14-fold, respectively. Previously, it had been shown that a trimethoprim resistance cartridge inserted into the *Xho*I site within *cbbR* blocked expression of the $cbb_I$ genes (16). Since the region of sequence between −280 bp (pVKB1) and −330 bp (pVKG1) was shown to play an important role in high-level expression of the $cbb_I$ operon, a 4-bp deletion, from −281 to −284 bp, was introduced into plasmid pVKG1, generating the deletion plasmid pVKG1ΔXho. *R. sphaeroides* HR::pVKG1ΔXho showed drastically reduced levels of *lacZ* expression compared to those observed for HR::pVKG1 under photoheterotrophic and photoautotrophic growth conditions, suggesting either that this sequence is position sensitive or that the *Xho*I site constitutes part of the activating (binding) sequence. A second potential UAS was located upstream of the *Pfl*MI site, since inclusion of an additional 306 bp of upstream sequence in plasmid pVKC1 resulted in slightly over a twofold increase in expression over that of pVKG1 under both photoheterotrophic and photoautotrophic growth conditions. The *Xho*I deletion was also introduced into plasmid pVKC1 to determine its effect on the more distal activating sequence. *R. sphaeroides* HR::pVKC1ΔXho also showed significant decreases in *lacZ* expression under photoheterotrophic and photoautotrophic growth conditions relative to that of the strain containing the parent fusion plasmid, HR::pVKC1. Interestingly, under photoheterotrophic and photoautotrophic conditions, *lacZ* expression in HR::pVKC1ΔXho was significantly higher than that of HR::pVKG1ΔXho, reinforcing the idea that a second UAS is present upstream of the *Pfl*MI site. The reduction in activity in HR::pVKC1ΔXho could be due to loss of the promoter-proximal activating sequence, suggesting that the more distal activating sequence is relatively insensitive to positional effects.

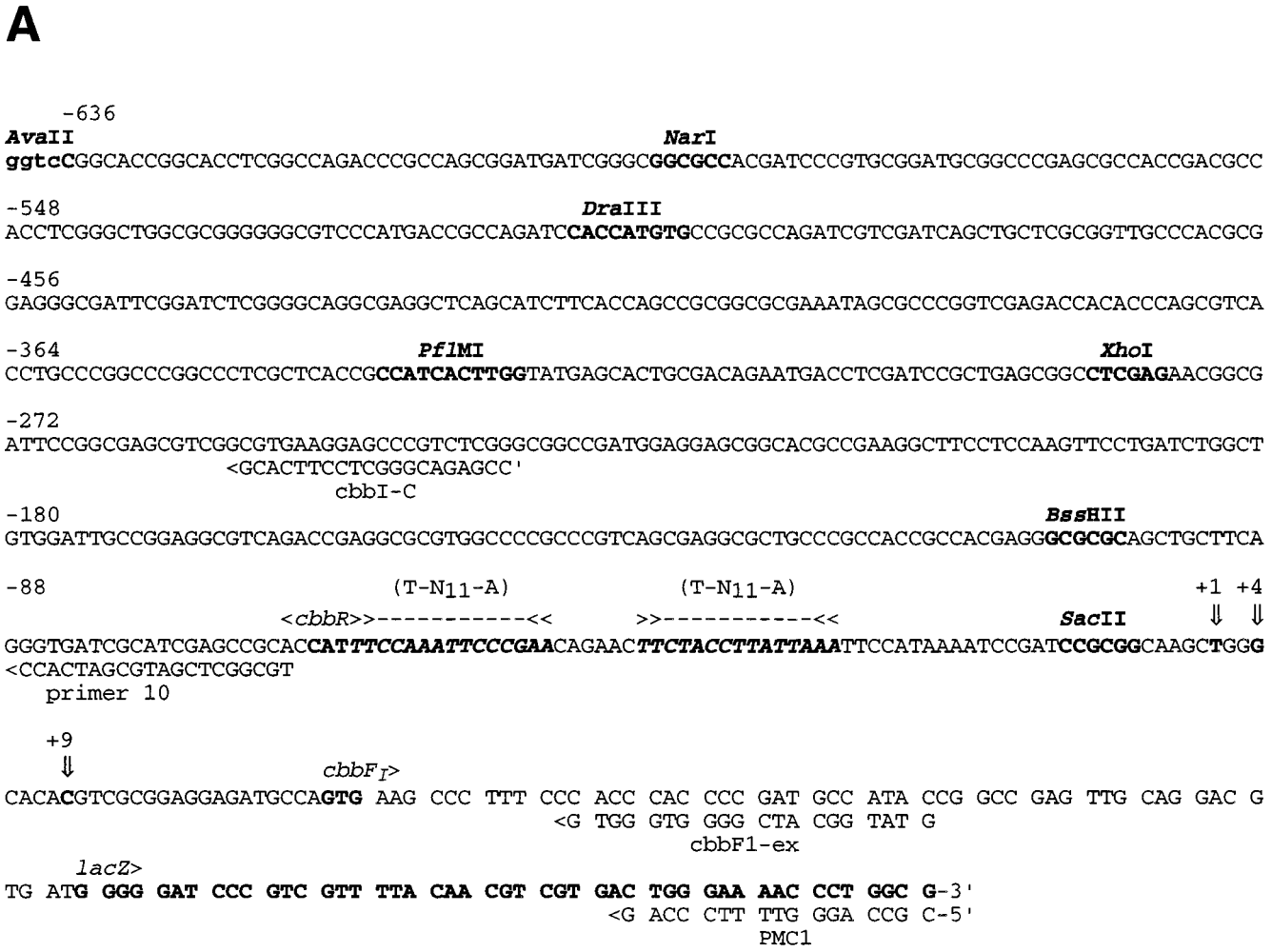


FIG. 1. Nucleotide sequence of the region used for construction of *cbbF*$_I$::*lacZ* translational fusion plasmid pVKC1. (A) The nucleotide sequence of the 718-bp *Ava*II fragment was used to construct plasmid pVKC1, spanning 571 bp of the *cbbR* gene, the *cbbR-cbbF*$_I$ intergenic region, and 57 bp of *cbbF*$_I$. Potential *cbbF*$_I$ mRNA start sites at +1 and +9 bp, as well as the +4-bp start site determined for the LacZ fusion pVKC1, are indicated by vertical arrows and are described in the text. The sequence is numbered relative to the distal mRNA start at +1 bp. Two imperfect inverted repeat sequences containing LysR-type binding motifs (T-$N_{11}$-A) are indicated. (B) Primer extension mapping of the *R. sphaeroides cbbF*$_I$ transcript 5′ endpoint(s). Shown are results of primer extension experiments with total RNA extracted from photoautotrophically grown *R. sphaeroides* HR (lane 1) and a synthetic oligonucleotide of the sequence 5′-GTATGGCATCGGGGTGGGTG-3′ (cbbF1-ex). The extension products are sized against a sequencing ladder with the same oligonucleotide primer and plasmid p12EH as template. The initiation points of the extension products are indicated by arrows.

RubisCO activity was also monitored during the course of each experiment (Fig. 2B, D, and F). RubisCO activities obtained for each of the fusion-containing strains displayed a normal pattern of RubisCO induction among the three growth regimens, indicating that the presence of the fusion plasmid did not interfere with normal *cbb* regulation. For a given growth condition, the RubisCO activities of the fusion strains showed some variability, which is consistent with the normal variability observed in measuring RubisCO activity in crude cell extracts.

**Regulation of *cbbF*$_I$*::lacZ* translational fusions pVKB1, pVKC1, and pVKC1ΔXho in *R. sphaeroides* CAC.** The presence or absence of $O_2$ appears to be an important regulatory signal for *cbb* expression in *R. sphaeroides* HR. *R. sphaeroides* CAC, a spontaneous mutant of *R. sphaeroides* HR, has gained the ability to grow chemoautotrophically under aerobic $CO_2$-fixing conditions in which the atmospheric $O_2$ concentration is as

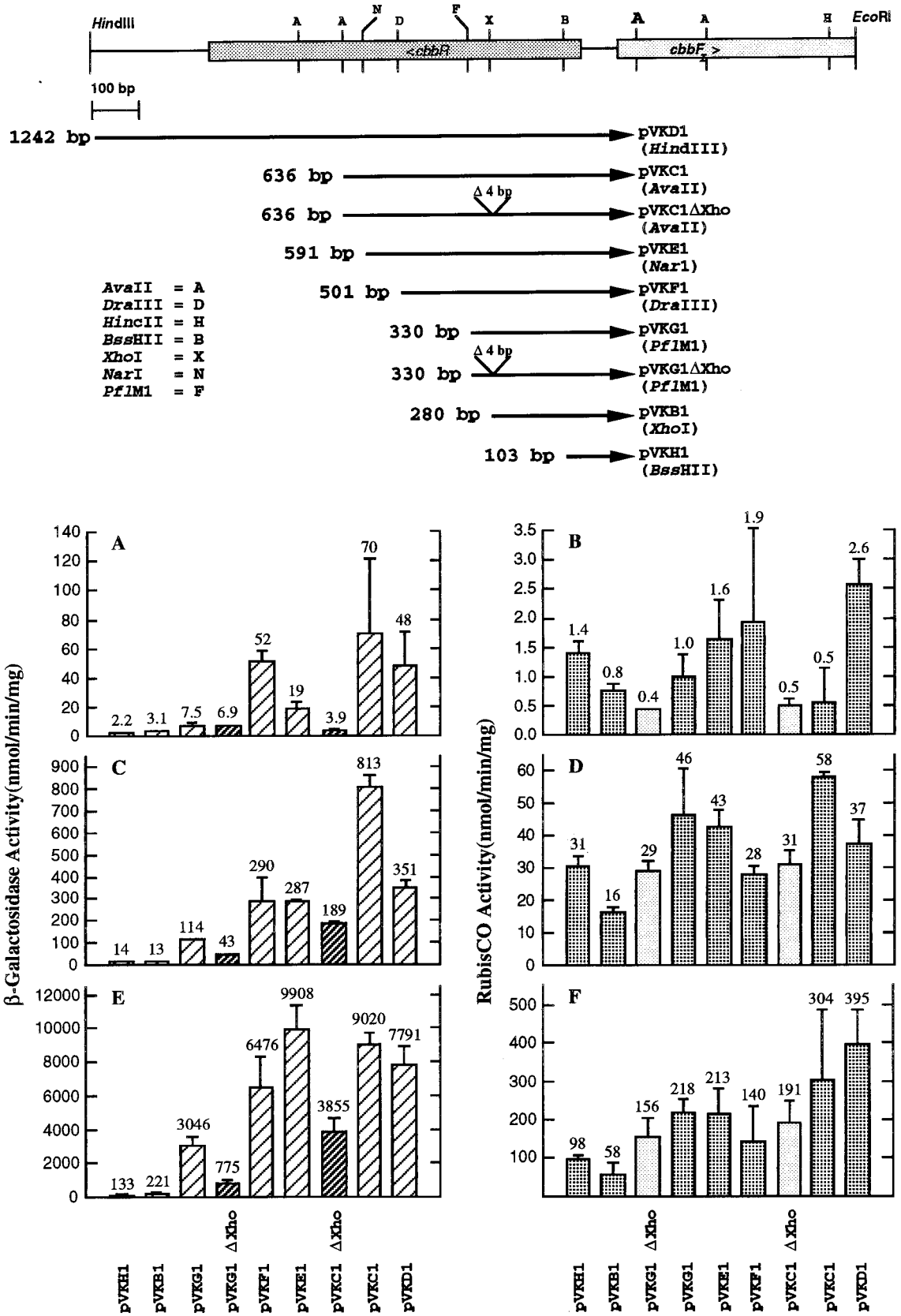


FIG. 2. β-Galactosidase and RubisCO assay results for *R. sphaeroides* HR::*lacZ*::*cbbF*$_I$ translational fusion strains. Maps depicting the sequences used to construct each fusion plasmid are shown. Multiple assays of several independent growth experiments were performed, and the standard deviations for each determination are denoted by the line above each bar. The average value for these determinations is also shown above each bar. The β-galactosidase (A, C, and E) and RubisCO (B, D, and F) activities for *R. sphaeroides* HR containing various *cbbF*$_I$::*lacZ* translational fusion plasmids grown under chemoheterotrophic (A and B), photoheterotrophic (C and D), and photoautotrophic (E and F) conditions are shown. The average β-galactosidase activities (two independent experiments) for the negative control strain HR::pVK1403 were 0.0 nmol/min/mg under chemoheterotrophic and photoheterotrophic growth conditions and 0.5 nmol/min/mg under photoautotrophic growth conditions. The average RubisCO activities for HR::pVK1403 were 1.0, 38, and 295 nmol/min/mg under chemoheterotrophic, photoheterotrophic, and photoautotrophic growth conditions, respectively.

TABLE 2. β-Galactosidase and RubisCO activities[a] in *R. sphaeroides* CAC and 1312, carrying various fusion plasmid constructs

| Strain and plasmid | Value for growth condition: | | | |
|---|---|---|---|---|
| | Chemoheterotrophy (malate-air) | Photoheterotrophy (malate-argon) | Photoautotrophy (1.5% $CO_2$–$H_2$) | Chemoautotrophy (5% $CO_2$–45% $H_2$–50% air) |
| CAC | | | | |
| pVKB1 | 3.9 (2.1) | 32 (46) | 467 (392) | 273 (82) |
| pVKC1 | 92 (1.3) | 1,079 (54) | 7,640 (332) | 12,635 (66) |
| pVKC1ΔXho | 25 (1.1) | 295 (48) | 3,192 (183) | 3,330 (73) |
| pVK1403 | 0.0 (1.5) | 3.0 (66) | 3.4 (338) | 0.0 (110) |
| 1312 | | | | |
| pVKH1 | 0.7 (1.8) | 2.5 (5.8) | No growth | |
| pVKB1 | 1.7 (2.1) | 2.7 (8.1) | No growth | |
| pVK1403 | 0.0 (2.0) | 0.2 (8.9) | No growth | |

[a] All enzyme activities are expressed in nanomoles per minute per milligram of protein. All values represent the averages of two to three independent determinations of multiple assays. Values in parentheses represent RubisCO activities in nanomoles of $CO_2$ fixed per minute per milligram of protein.

high as 10% (i.e., in minimal medium bubbled with 5% $CO_2$–45% $H_2$–50% air) (31). We examined $cbb_I$ expression in this strain in order to determine if the $cbb_I$ promoter is regulated normally under chemoheterotrophic, photoheterotrophic, and photoautotrophic conditions. We also wanted to determine if the same regulatory regions important for $cbb_I$ regulation in strain HR are necessary for $cbb_I$ expression under aerobic chemoautotrophic growth conditions. The regulation of *lacZ* expression from pVKB1, pVKC1, and pVKC1ΔXho was examined in *R. sphaeroides* CAC grown under chemoheterotrophic, photoheterotrophic, and photoautotrophic conditions as well as under chemoautotrophic aerobic $CO_2$-fixing conditions (i.e., in minimal medium bubbled with 5% $CO_2$–45% $H_2$–50% air). In general, the pattern of regulation and the levels of β-galactosidase expression observed for CAC::pVKC1, CAC::pVKB1, and CAC::pVKC1ΔXho were comparable to results obtained with these plasmids in *R. sphaeroides* HR (Table 2). The upstream activating region 5′ to −280 bp functions normally in *R. sphaeroides* CAC. As was the case in *R. sphaeroides* HR, the absolute level of *lacZ* expression from CAC::pVKC1 was significantly higher than that obtained for CAC::pVKB1 under all the growth conditions tested. In CAC::pVKC1ΔXho, the level of *lacZ* expression under each of the growth conditions was intermediate between those of CAC::pVKB1 and CAC::pVKC1. $O_2$ did not negatively regulate the $cbb_I$ promoter under aerobic $CO_2$-fixing conditions. When strains were grown under chemoautotrophic conditions, *lacZ* expression in CAC::pVKC1, CAC::pVKB1, and CAC::pVKC1ΔXho was comparable to that observed for the same strain grown photoautotrophically. This result also indicates that, in *R. sphaeroides* CAC, the upstream activating region is also necessary for maximal $cbb_I$ expression under chemoautotrophic growth. The RubisCO activities determined for each of these strains were similar to those determined for *R. sphaeroides* HR carrying the same plasmids. The lower level of RubisCO activity under chemoautotrophic conditions than under photoautotrophic growth conditions reflects the fact that the level of $CO_2$ and $O_2$ supplied to these cells was not optimized in these experiments (31a).

**Regulation of the $cbbF_I$::*lacZ* translational fusion plasmids in the *cbbR* insertion mutant *R. sphaeroides* 1312.** In order to explore the role that the *trans*-acting transcriptional activator *cbbR* plays in $cbb_I$ operon regulation, the $cbbF_I$ fusion plasmids pVKH1 and pVKB1 were introduced into the *cbbR* insertion mutant, *R. sphaeroides* 1312 (Table 2). This strain contains an inactivated *cbbR* gene generated via the insertion of a trimethoprim resistance cartridge within the *cbbR* coding sequence at the *Xho*I site at −280 bp. This strain does not express form I RubisCO and expresses form II RubisCO at a low level compared to that of wild-type strain HR. Strain 1312 is capable of growth under chemoheterotrophic and photoheterotrophic conditions but not under photoautotrophic conditions (16). The results of these experiments indicate that *cbbR* is necessary for regulated expression in 1312::pVKH1 and 1312::pVKB1, as no induction of β-galactosidase was observed under photoheterotrophic conditions. We were not able to analyze fusion plasmids that contained sequences beyond the *Xho*I site in strain 1312 due to the fact that these plasmids underwent rapid recombination with the chromosome to regenerate *cbbR*.

**Binding of CbbR to the $cbb_I$ promoter.** The *R. sphaeroides* HR *cbbR* gene was placed under the control of a phage T7 promoter via cloning into the expression plasmid pET11a (7), forming the CbbR expression plasmid pET11R-11. This plasmid was then transformed into *E. coli* BL21(DE3) (35). This strain [BL21(DE3)::pET11R-11] produced an IPTG-inducible protein of approximately 35 kDa (data not shown). N-terminal sequencing showed the first 10 amino acids of this protein to be identical to the deduced sequence for *R. sphaeroides* HR CbbR. Gel mobility shift assays were performed with extracts of IPTG-induced cultures of BL21(DE3)::pET11R-11 and a $cbb_I$ promoter probe consisting of the 190-bp *Bss*HII-*Bam*HI fragment of pKC1-5 (Fig. 3A). Promoter binding activity was detected as a single shifted band and was sensitive to both boiling and proteinase K treatment (Fig. 3B, lanes 2 to 4). No binding activity was detected in binding assay mixtures containing either no protein (Fig. 3B, lane 1) or an equivalent amount of extract of *E. coli* BL21(DE3) containing the parent vector pET11a (Fig. 3B, lane 9). Competition with a 100-fold excess of cold probe DNA resulted in the loss of the shifted signal, while addition of a 200-fold excess of salmon sperm DNA had no effect (Fig. 3B, lanes 5 and 6). In order to further narrow down the site of CbbR binding, the 92-bp *Bss*HII-*Sac*II and 98-bp *Sac*II-*Bam*HI fragments of pKC1-5 were used as competitors in gel mobility shift assays. Addition of a 100-fold molar excess of the 92-bp *Bss*HII-*Sac*II fragment resulted in the disappearance of the shifted band (Fig. 3B, lane 7), while the addition of a 100-fold molar excess of the 98-bp *Sac*II-*Bam*HI fragment had no effect (Fig. 3B, lane 8). This indicates that CbbR binds the $cbb_I$ promoter somewhere between 9 and 100 bp 5′ to the $cbbF_I$ transcription start. Gel mobility shift experiments with restriction fragments spanning up to 636 bp of sequence upstream of the $cbbF_I$ transcription start detected no additional CbbR binding sites (data not shown).

A

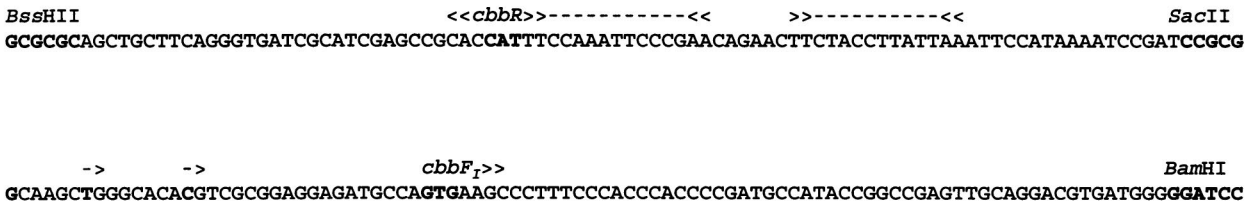


B

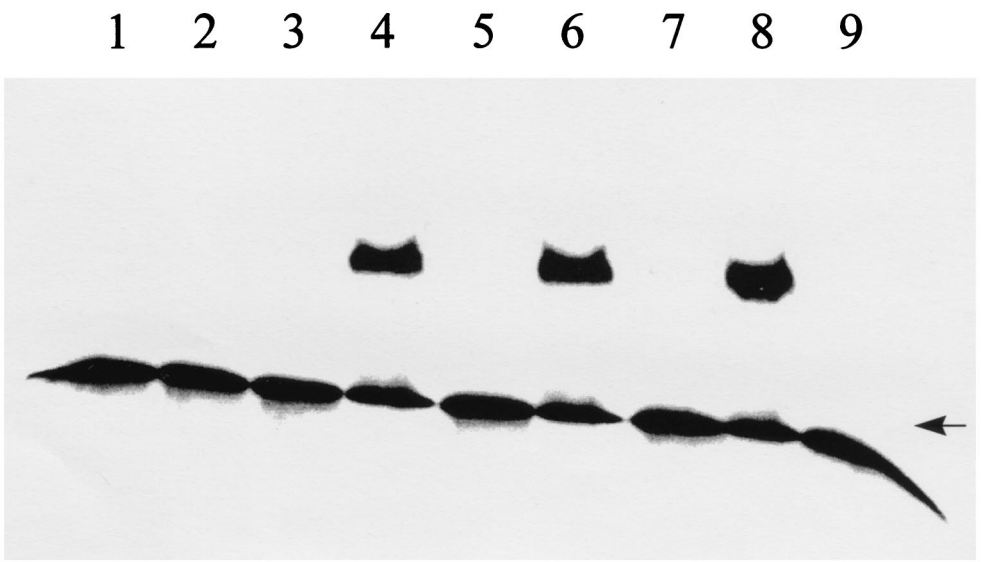


FIG. 3. Binding of CbbR to the $cbb_I$ promoter. Shown is the phosphorimage of a gel mobility shift assay (B) with the 190-bp *Bss*HII-*Bam*HI fragment (A) of pKC1-5 as a probe and extracts (2 μg) of BL21(DE3) containing either pET11R-11 (11R) or pET11a (11A). Lane 1, no extract added; lane 2, 11R plus 5 min of incubation at 100°C; lane 3, 11R plus proteinase K; lane 4, 11R; lane 5, 11R plus 100-fold molar excess of unlabeled probe; lane 6, 11R plus 200-fold excess of salmon sperm DNA; lane 7, 11R plus 100-fold molar excess of the 92-bp *Bss*HII-*Sac*II fragment; lane 8, 11R plus 100-fold molar excess of the 98-bp *Sac*II-*Bam*HI fragment; lane 9, 11A. All binding reaction mixtures contained 3 μg of poly(dI-dC) · poly(dI-dC). The arrow indicates the position of the unbound DNA (B). Putative CbbR binding sites (>>---<<) and transcription start sites (->) are indicated (A). The phosphorimage was generated with a Storm 840 PhosphorImager in conjunction with ImageQuant version 4.2 software (Molecular Dynamics, Inc.).

## DISCUSSION

The results of expression studies with $cbb_I$::*lacZ* promoter fusions indicated that 103 bp (plasmid pVKH1) of sequence 5′ to the *R. sphaeroides* HR $cbbF_I$ transcription start is sufficient to support detectable levels of regulated $cbb_I$ expression (i.e., low levels under chemoheterotrophic conditions, intermediate levels under photoheterotrophic conditions, and high levels under photoautotrophic conditions). This level of promoter activity is relatively unchanged with the addition of up to 280 bp of upstream sequence (plasmid pVKB1). Regulated expression from this region is dependent on the presence of an intact *cbbR* gene, since 1312::pVKH1 and 1312::pVKB1 cells grown in malate medium under aerobic or anaerobic growth conditions exhibited no differences in *lacZ* expression. These results suggested that the 103 bp of sequence 5′ to $cbbF_I$, which spans the *cbbR-ccbF*$_I$ intergenic region, contains regulatory sites necessary for CbbR-mediated regulation of the $cbb_I$ operon promoter. Gel mobility shift binding assays show that CbbR does bind within this stretch of sequence between 9 and 100 bp 5′ to the $cbbF_I$ transcription start. This region contains two imperfect inverted repeat elements, each of which contains the CbbR/LysR-type consensus binding motif T-$N_{11}$-A (18). These T-$N_{11}$-A motifs probably represent the site of CbbR binding, as they show a high degree of sequence similarity with the corresponding region of the *X. flavus cbb* promoter (Fig. 4), in which the T-$N_{11}$-A motifs are known to bind CbbR (40, 41). This arrangement of duplicated T-$N_{11}$-A sequences occurs within the intergenic regions between the divergently transcribed *cbbR* gene and the *cbb* operons of a number of phototrophic and autotrophic bacteria (24, 30, 41, 46). In the autotrophic bacteria *T. ferrooxidans* and *R. eutropha*, CbbR (or RbcR) has also been shown to bind specifically to a similar region of dyad symmetry containing two T-$N_{11}$-A repeats (24, 25). Mutations within this region of dyad symmetry in *T. ferrooxidans* reduced the ability of RbcR to bind in vitro (24).

In *R. sphaeroides* HR, our $cbb_I$::*lacZ* promoter fusion results indicate the presence of sequence elements upstream of −103 bp that exert a positive effect on $cbb_I$ promoter function under

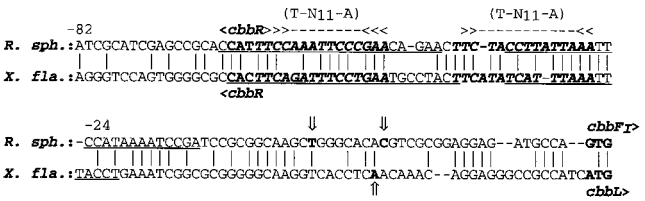


FIG. 4. Comparison of the *cbbF*$_I$-*cbbR* intergenic region of *R. sphaeroides* with that of the *X. flavus cbb* operon. Vertical arrows represent mapped putative transcription start sites. Vertical lines represent nucleotides conserved between the two sequences. Putative CbbR binding sites (>>---<<) in the *R. sphaeroides* sequence are indicated. The underlined sequence is the site of CbbR binding to the *X. flavus cbbL* promoter. Hyphens indicate gaps inserted to maximize sequence identity. Bold-face italic sequences are mentioned in the text. Numbers refer to the distance upstream from the transcription start of *R. sphaeroides* *cbbF*$_I$.

all growth conditions tested. The positive regulatory region resides, roughly, between −280 bp (pVKB1) and −636 bp (pVKC1) and is probably made up of at least two elements or UASs. The first promoter-proximal UAS is found either within or overlapping the 50-bp sequence between −280 bp (pVKB1) and −330 bp (pVKG1) and accounts for the majority of the observed enhancement under photoheterotrophic and photoautotrophic conditions (9- and 14-fold, respectively). The second promoter-distal UAS is probably located between −330 bp (pVKG1) and −636 bp (pVKC1). The presence of two UASs is suggested by the results obtained when the same 4-bp *Xho*I deletion (−281 to −284 bp) is introduced into pVKC1 and pVKG1, yielding pVKC1ΔXho and pVKG1ΔXho, respectively. In both cases the *Xho*I deletion results in a sharp decrease in expression. If the *Xho*I deletion disrupts a site that is solely responsible for the enhancement of *cbb*$_I$ expression, then the *lacZ* expression levels for pVKC1ΔXho and pVKG1ΔXho would be expected to be similar. This is not the case. Under photoheterotrophic and photoautotrophic growth conditions, the presence of the 306 bp of additional sequence upstream in pVKC1ΔXho results in a four- to fivefold increase in *lacZ* expression relative to that in pVKG1ΔXho. These results indicate that the promoter-distal region plays a role in *cbb*$_I$ activation.

*R. sphaeroides* CAC (for chemoautotrophic competent) is a variant of *R. sphaeroides* HR that has gained the capacity to grow as a chemoautotroph by using $CO_2$ as sole carbon source, $H_2$ as an electron donor, and $O_2$ as a terminal electron acceptor (31). The fact that this strain expresses RubisCO at high levels in the presence of $O_2$ led us to introduce the *cbb*$_I$::*lacZ* fusion plasmids pVKB1, pVKC1ΔXho, and pVKC1 into strain CAC in order to determine if this strain showed any alterations in *cbb*$_I$ expression. The *lacZ* expression levels for each strain, grown chemoheterotrophically, photoheterotrophically, and photoautotrophically, were consistent with those determined in strain HR. Thus, the same expression-enhancing effect of the region upstream of −280 bp was noted. The *lacZ* expression levels for each of the plasmid-containing strains, grown under aerobic chemoautotrophic conditions, indicate that this promoter is not subject to negative oxygen regulation under these growth conditions. The results also suggest that the mutation that allows *R. sphaeroides* CAC to grow chemoautotrophically is probably not a mutation in the *cbb*$_I$ promoter.

The basis for the observed expression-enhancing effect of sequences upstream of bp position −280 is unknown. We could detect no additional mRNA start points near this region that would indicate the presence of a second promoter. The enhancement is more likely due to the presence of additional binding sites for a positive regulatory factor(s) acting on the downstream promoter. It seems unlikely that CbbR binds to the UASs, as we were unable to detect CbbR binding to this region in gel mobility shift assays. One potential candidate for this role is the response regulator (RegA/PrrA) of the two-component regulatory system RegB/PrrB-RegA/PrrB, which has previously been implicated in activation of *cbb* expression (33). Joint transcriptional control of gene expression by a two-component response regulatory system and a LysR-type transcriptional activator has previously been observed for *xpsR* in *Ralstonia solanacearum* (21). As with the *cbb*$_I$ promoter, the *xpsR* promoter consists of a promoter-proximal region, within 117 bp of *xpsR*, that confers low-level regulated expression and binds the LysR-type transcriptional activator PhcA. An additional 14-bp upstream element, centered at 315 bp 5′ to *xpsR*, is necessary for full activation of expression and is dependent on the response regulator VsrD.

Unlike with other *cbb* operons previously studied, our results firmly establish that there is an additional regulatory domain distal to *cbbF*$_I$ that functions to enhance *cbb*$_I$ promoter activity under all growth conditions tested. Work to identify those sequences in each domain responsible for the observed regulation as well as to characterize the binding sites for CbbR is now under way.

## ACKNOWLEDGMENTS

We thank D. A. Bryant for plasmid pMC1403 and J. L. Gibson for help in editing the manuscript.

This work was supported by Public Health Service grant GM 45404 from the National Institutes of Health.

## REFERENCES

1. **Ausubel, F. M., R. Brent, R. E. Kingston, D. D. Moore, J. G. Seidman, J. A. Smith, and K. Struhl.** 1987. Current protocols in molecular biology, vol. 1. John Wiley and Sons, Inc., New York, N.Y.
2. **Bishop, R. E., and J. H. Weiner.** 1993. Overproduction, solubilization, purification and DNA-binding properties of AmpR from *Citrobacter freundii*. Eur. J. Biochem. **213:**405–412.
3. **Cantrell, A., and D. A. Bryant.** 1987. Molecular cloning and nucleotide sequence of the *psaA* and *psaB* genes of the cyanobacterium *Synechococcus* sp. PCC 7002. Plant Mol. Biol. **9:**453–468.
4. **Chen, J.-H., J. L. Gibson, L. A. Macue, and F. R. Tabita.** 1991. Identification, expression, and deduced primary structure of transketolase and other enzymes encoded within the form II $CO_2$ fixation operon of *Rhodobacter sphaeroides*. J. Biol. Chem. **266:**20447–20452.
5. **Davis, J., T. J. Donohue, and S. Kaplan.** 1988. Construction, characterization, and complementation of a Puf$^-$ mutant of *Rhodobacter sphaeroides*. J. Bacteriol. **170:**320–329.
6. **Dubbs, J. M., and D. A. Bryant.** 1991. Molecular cloning and transcriptional analysis of the *cpeBA* operon of the cyanobacterium *Pseudanabaena* sp. PCC 7409. Mol. Microbiol. **5:**3073–3085.
7. **Dubendorff, J. W., and F. W. Studier.** 1991. Controlling basal expression in an inducible T7 expression system by blocking the target T7 promoter with *lac* repressor. J. Mol. Biol. **219:**45–59.
8. **Falcone, D. L., and F. R. Tabita.** 1991. Expression of endogenous and foreign ribulose 1,5-bisphosphate carboxylase-oxygenase (RubisCO) genes in a RubisCO deletion mutant of *Rhodobacter sphaeroides*. J. Bacteriol. **173:** 2099–2108.
9. **Falcone, D. L., R. G. Quivey, Jr., and F. R. Tabita.** 1988. Transposon mutagenesis and physiological analysis of a strain containing inactivated form I and form II ribulose bisphosphate carboxylase/oxygenase genes in *Rhodobacter sphaeroides*. J. Bacteriol. **170:**5–11.
10. **Falcone, D. L., and F. R. Tabita.** 1993. Complementation analysis and regulation of $CO_2$ fixation gene expression in a ribulose-1,5-bisphosphate carboxylase-oxygenase deletion strain of *Rhodospirillum rubrum*. J. Bacteriol. **175:**5066–5077.
11. **Figurski, D., and D. R. Helinsky.** 1979. Replication of an origin-containing derivative of the plasmid RK2 dependent on a plasmid function provided *in trans*. Proc. Natl. Acad. Sci. USA **76:**1648–1652.
12. **Gibson, J. L.** 1995. Genetic analysis of $CO_2$ fixation genes, p. 1107–1124. *In* R. E. Blankenship, M. T. Madigan, and C. E. Bauer (ed.), Anoxygenic photosynthetic bacteria. Kluwer Academic Publishers, Dordrecht, The Netherlands.
13. **Gibson, J. L., and F. R. Tabita.** 1977. Different molecular forms of ribulose-

1,5-bisphosphate carboxylase from *Rhodopseudomonas sphaeroides*. J. Biol. Chem. **252:**943–949.
14. **Gibson, J. L., H.-J. Chen, P. A. Tower, and F. R. Tabita.** 1990. The form II fructose-1,6-bisphosphatase and phosphoribulokinase genes form part of a large operon in *Rhodobacter sphaeroides*: primary structure and insertional mutagenesis. Biochemistry **29:**8085–8093.
15. **Gibson, J. L., D. L. Falcone, and F. R. Tabita.** 1991. Nucleotide sequence, transcriptional analysis and expression of genes encoded within the form I $CO_2$ fixation operon of *Rhodobacter sphaeroides*. J. Biol. Chem. **266:**14646–14653.
16. **Gibson, J. L., and F. R. Tabita.** 1993. Nucleotide sequence and functional analysis of CbbR, a positive regulator of the Calvin cycle operons of *Rhodobacter sphaeroides*. J. Bacteriol. **175:**5778–5784.
17. **Gibson, J. L., and F. R. Tabita.** 1996. The molecular regulation of the reductive pentose phosphate pathway in proteobacteria and cyanobacteria. Arch. Microbiol. **166:**141–150.
18. **Goethals, K., M. Van Montague, and M. Holsters.** 1992. Conserved motifs in a divergent *nod* box of *Azorhizobium caulinodans* ORS571 reveal a common structure in promoters regulated by LysR-type proteins. Proc. Natl. Acad. Sci. USA **89:**1646–1650.
19. **Hallenbeck, P. L., R. Lerchen, P. Hessler, and S. Kaplan.** 1990. Roles of CfxA, CfxB, and external electron acceptors in regulation of ribulose 1,5-bisphosphate carboxylase/oxygenase in *Rhodobacter sphaeroides*. J. Bacteriol. **172:**1736–1748.
20. **Hallenbeck, P. L., R. Lerchen, P. Hessler, and S. Kaplan.** 1990. Phosphoribulokinase activity and regulation of $CO_2$ fixation critical for photosynthetic growth of *Rhodobacter sphaeroides*. J. Bacteriol. **172:**1749–1761.
21. **Jianzhong, H., W. Yindeeyoungyeon, R. P. Garg, T. P. Denny, and M. A. Schell.** 1998. Joint transcriptional control of *xpsR*, the unusual signal integrator of the *Ralstonia solanacearum* virulence gene regulatory network, by a response regulator and a LysR-type transcriptional activator. J. Bacteriol. **180:**2736–2743.
22. **Jouanneau, Y., and F. R. Tabita.** 1986. Independent regulation of synthesis of form I and form II ribulose bisphosphate carboxylase-oxygenase in *Rhodopseudomonas sphaeroides*. J. Bacteriol. **165:**620–624.
23. **Knauf, V. C., and W. N. Nester.** 1982. Wide host range cloning vectors: a cosmid clone bank of an *Agrobacterium* Ti plasmid. Plasmid **8:**45–54.
24. **Kusano, T., and K. Sugawara.** 1993. Specific binding of *Thiobacillus ferrooxidans* RbcR to the intergenic sequence between the *rbc* operon and the *rbcR* gene. J. Bacteriol. **175:**1019–1025.
25. **Kusian, B., and B. Bowein.** 1995. Operator binding of the CbbR protein, which activates the duplicate *cbb* $CO_2$ assimilation operons of *Alcaligenes eutrophus*. J. Bacteriol. **177:**6568–6574.
26. **Madigan, M. T., and H. Gest.** 1979. Growth of the photosynthetic bacterium *Rhodopseudomonas capsulata* chemoautotrophically in the darkness with $H_2$ as the energy source. J. Bacteriol. **137:**524–530.
27. **Maniatis, T., E. F. Fritsch, and J. Sambrook.** 1982. Molecular cloning: a laboratory manual. Cold Spring Harbor Laboratory Press, Cold Spring Harbor, N.Y.
28. **Meijer, W., A. C. Arnberg, H. G. Enequist, P. Terpstra, M. E. Lindstrom, and L. Dijkhuizen.** 1991. Identification and organization of carbon dioxide fixation genes in *Xanthobacter flavus* H4-14. Mol. Gen. Genet. **225:**320–330.
29. **Omerod, J. G., K. D. Omerod, and H. Gest.** 1961. Light dependent utilization of organic compounds and photoproduction of hydrogen by photosynthetic bacteria: relationship with nitrogen metabolism. Arch. Biochem. Biophys. **94:**449–463.
30. **Paoli, G. C., S. M. Morgan, F. R. Tabita, and J. M. Shively.** 1995. Expression of the *cbbLcbbS* and *cbbM* genes and distinct organization of the *cbb* Calvin cycle structural genes of *Rhodobacter capsulatus*. Arch. Microbiol. **164:**396–405.
31. **Paoli, G. C., and F. R. Tabita.** 1998. Aerobic lithoautotrophic growth and RubisCO function in *Rhodobacter capsulatus* and a spontaneous gain of function mutant of *Rhodobacter sphaeroides*. Arch. Microbiol. **170:**8–17.
31a. **Paoli, G. C., and F. R. Tabita.** Unpublished results.
32. **Pridmore, R. D.** 1987. New and versatile cloning vectors with kanamycin resistance marker. Gene **56:**309–312.
33. **Qian, Y., and F. R. Tabita.** 1996. A global signal transduction system regulates aerobic and anaerobic $CO_2$ fixation in *Rhodobacter sphaeroides*. J. Bacteriol. **178:**12–18.
34. **Shapira, S. K., J. Chou, F. V. Richaud, and M. J. Casadaban.** 1983. New versatile plasmid vectors for expression of hybrid proteins coded by a cloned gene fused to *lacZ* gene sequences encoding an enzymatically active carboxy-terminal portion of β-galactosidase. Gene **25:**71–82.
35. **Studier, F. W., A. H. Rosenberg, J. J. Dunn, and J. W. Dubendorff.** 1990. Use of T7 RNA polymerase to direct expression of cloned genes. Methods Enzymol. **185:**60–89.
36. **Suwanto, A., and S. Kaplan.** 1989. Physical and genetic mapping of the *Rhodobacter sphaeroides* genome: presence of two unique circular chromosomes. J. Bacteriol. **171:**5858–5859.
37. **Suwanto, A., and S. Kaplan.** 1992. Chromosome transfer in *Rhodobacter sphaeroides*: Hfr formation and genetic evidence for two unique circular chromosomes. J. Bacteriol. **174:**1135–1145.
38. **Tabita, F. R.** 1988. Molecular and cellular regulation of autotrophic carbon dioxide fixation in microorganisms. Microbiol. Rev. **52:**155–189.
39. **Tabita, F. R.** 1995. The biochemistry and metabolic regulation of carbon metabolism and $CO_2$ fixation in purple bacteria, p. 885–914. *In* R. E. Blankenship, M. T. Madigan, and C. E. Bauer (ed.), Anoxygenic photosynthetic bacteria. Kluwer Academic Publishers, Dordrecht, The Netherlands.
40. **van den Berg, E. R. E., L. Dijkhuizen, and W. G. Meijer.** 1993. CbbR, a LysR-type transcriptional activator, is required for expression of the autotrophic $CO_2$ fixation enzymes of *Xanthobacter flavus*. J. Bacteriol. **175:**6097–6104.
41. **van Keulen, G., L. Girbal, E. R. van den Berg, L. Dijkhuizen, and W. G. Meijer.** 1998. The LysR-type transcriptional regulator CbbR controlling autotrophic $CO_2$ fixation by *Xanthobacter flavus* is an NADPH sensor. J. Bacteriol. **180:**1411–1417.
42. **Viale, A. M., H. Kobayashi, T. Akazawa, and S. Henikoff.** 1991. *rbcR*, a gene coding for a member of the LysR family of transcriptional regulators, is located upstream of the expressed set of ribulose-1,5-bisphosphate carboxylase/oxygenase genes in the photosynthetic bacterium *Chromatium vinosum*. J. Bacteriol. **173:**5224–5229.
43. **Wang, X., D. L. Falcone, and F. R. Tabita.** 1993. Reductive pentose phosphate-independent $CO_2$ fixation in *Rhodobacter sphaeroides* and evidence that ribulose bisphosphate carboxylase/oxygenase activity serves to maintain the redox balance of the cell. J. Bacteriol. **175:**3372–3379.
44. **Weaver, K. E., and F. R. Tabita.** 1983. Isolation and partial characterization of *Rhodopseudomonas sphaeroides* mutants defective in regulation of ribulose bisphosphate carboxylase/oxygenase. J. Bacteriol. **156:**507–515.
45. **Whitman, W., and F. R. Tabita.** 1976. Inhibition of ribulose 1,5-bisphosphate carboxylase by pyridoxal 5-phosphate. Biochem. Biophys. Res. Commun. **71:**1034–1039.
46. **Windhovel, U., and B. Bowein.** 1991. Identification of *cfxR*, an activator gene of autotrophic $CO_2$ fixation in *Alcaligenes eutrophus*. Mol. Microbiol. **5:**2695–2705.
47. **Yanisch-Perron, C., J. Vieira, and J. Messing.** 1985. Improved M13 phage cloning vectors and host strains: nucleotide sequences of the M13mp18 and pUC19 vectors. Gene **33:**103–119.